International Journal of Thermophysics, Vol. 23, No. 6, November 2002 (© 2002)

Measurement of Speed of Sound with a Spherical Resonator: HCFC-22, HFC-152a, HFC-143a, and Propane

M. G. He,[1,2] Z. G. Liu,[1] and J. M. Yin[1]

Received January 14, 2002

A spherical resonator and acoustic signal measurement apparatus have been designed and developed for measuring the speed of sound in the gaseous phase. The inner radius of the spherical resonator, being about 6.177 cm, was determined by measuring the speed of sound in gaseous argon at temperatures between 293 and 323 K and at pressures up to 200 kPa. Measurements of the speed of sound in four halogenated hydrocarbons are presented, the compounds are chlorodifluoromethane ($CHClF_2$ or HCFC-22), 1,1-difluoroethane (CH_3CHF_2 or HFC-152a), 1,1,1-trifluoroethane (CH_3CF_3 or HFC-143a), and propane ($CH_3CH_2CH_3$ or HC-290). Ideal-gas heat capacities and acoustic virial coefficients were directly deduced from the present data. The results were compared with those from other studies. In this work, the experimental uncertainties in temperature, pressure, and speed of sound are estimated to be less than ± 14 mK, ± 2.0 kPa, and $\pm 0.0037\%$, respectively. In addition, equations for the ideal-gas isobaric specific heat capacity for HFC-152a, HFC-143a, and propane are proposed, which are applicable in temperature ranges 240 to 400 K for HFC-152a, 250 to 400 K for HFC-143a, 225 to 375 K for propane. The purities for each of the samples of HCFC-22, HFC-152a, HFC-143a, and propane are better than 99.95 mass%.

KEY WORDS: HCFC-22; HFC-152a; HFC-143a; ideal-gas specific heat capacity; propane; refrigerant; second acoustic virial coefficient; speed of sound; spherical acoustic resonator.

1. INTRODUCTION

The properties of chlorofluorocarbon (CFC) alternatives have been studied since the mid-1970s after publication of Rowland and Molina's paper on

[1] Division of Thermodynamics and Heat Transfer, School of Energy and Power Engineering, Xi'an Jiaotong University, Xi'an, Shaanxi 710049, People's Republic of China.
[2] To whom correspondence should be addressed. E-mail: mghe@mail.xjtu.edu.cn

0195-928X/02/1100-1599/0 © 2002 Plenum Publishing Corporation

ozone layer depletion potential by chlorofluoro-carbons (CFCs) [1]. The Montreal Protocol Agreement of September 1987 limited production of specified chlorofluorocarbons and hydrochlorofluorocarbons, such as CFC-12, HCFC-22, etc. The Kyoto Protocol announced in May 1998 would limit the discharge of gases with significant global warming potential. Obviously, the protocols would accelerate the study of CFC alternatives. Many of the studies have shown that HFC-152a, HFC-143a, and propane are thought to be important components of mixtures proposed as alternatives to refrigerants CFC-12 and/or HCFC-22. It is essential to study the thermodynamic properties of these compounds.

The thermodynamic properties of refrigerants in the gaseous phase are fundamental information needed to reveal the thermodynamic characteristics of refrigerants as applied in various energy conversion systems. For example, in order to calculate thermal properties such as enthalpy and entropy from the equation of state, the value of the ideal-gas specific heat capacity is needed. The measurement of speed of sound with a spherical acoustic resonator is recognized as one of the most accurate approaches for determining the thermophysical properties of dilute gases [2]. Many important thermophysical properties, such as the ideal gas heat capacity, thermal conductivity, viscosity, etc., can be deduced from accurate speed of sound values [2]. The measurement of speed of sound with a spherical acoustic resonator has been established in U.S.A, United Kingdom, Germany, and Japan [3–6]. Our group has carried out many studies on the thermophysical properties of alternative refrigerants [7], and proposed a refrigerant mixture HFC-152a/HCFC-22 to replace CFC-12 which is widely used in refrigerators in China [8]. Our laboratory had developed a spherical resonator and acoustic signal measurement apparatus in 1999 [9], and speeds of sound and ideal-gas specific heat capacities of the mixture HFC-152a/HCFC-22 had been measured [10]. In this paper, we have measured 24 speeds of sound in gaseous HCFC-22, 24 speeds of sound in gaseous HFC-152a, 28 speeds of sound in gaseous HFC-143a, and 24 speeds of sound in gaseous propane at temperature between 293 and 313 K and at pressures up to 200 kPa by means of the spherical acoustic resonator. The ideal-gas isobaric specific heat capacities as well as the second acoustic virial coefficients have been derived from the present speed-of-sound measurements.

2. PRINCIPLE OF MEASUREMENT

A detailed description on the theory and experimental development of spherical acoustic resonators was given by Moldover and Mehl [11], who

reported the universal gas constant with the highest accuracy as $8.314471 \pm 0.000014\ \mathrm{J \cdot mol^{-1} \cdot K^{-1}}$ based on the measurement of the speed of sound in argon.

A stable acoustic field composed of a series of standing waves was formed in a spherical cavity filled by the measured gas, when a stable sinusoidal wave was excited. The velocity potential $\psi(r)$ of this acoustic field satisfies the Hemholtz equation:

$$(\nabla^2 + k^2) \cdot \psi(r) = 0 \tag{1}$$

where $k = \omega/u$, ω is the angular frequency, $\omega = 2\pi f$, f is the frequency, and u is the speed of sound. The boundary condition of Eq. (1) in an ideal rigid spherical cavity is expressed as

$$\left.\frac{dj_l(kr)}{d(kr)}\right|_{r=a} = 0 \tag{2}$$

where a is the radius of the spherical cavity, $j_l(kr)$ is the lth-order spherical Bessel function. $v_{l,s} = k_{l,s}a$ is the sth solution of Eq. (2), and $k_{l,s}$ is an eigenvalue of Eq. (1). The values of $v_{l,s}$ used in the present study are as follow: $v_{0,2} = 4.493409$, $v_{0,3} = 7.725252$, $v_{0,4} = 10.904122$, $v_{0,5} = 14.066194$, and $v_{0,6} = 17.220755$. Those for which $l = 0$ are the radially symmetric modes. Obviously, the speed of sound of the filled gas is

$$u = \frac{\omega_{0,s}}{k_{0,s}} = \frac{2\pi f_{0,s} a}{v_{0,s}} \tag{3}$$

As illustrated in Fig. 1, the resonator wave was generated by a transducer driven by a frequency synthesizer, and was detected by another transducer accompanied by a transient measurement analysis instrument. In a practical spherical resonator, the attenuation of the resonator wave exists because of the non-ideal factor. In this case, the resonant frequency $\mathsf{F} = f_{0,s} - ig_{0,s}$ indicated by a complex number may be expressed by [12]

$$u + iv = \frac{d}{g + i(f_S - \mathsf{F})} + b_1 + ib_2 \tag{4}$$

where $u + iv$ is the complex expression of amplitude of the detected wave, d is the ratio of the source output and detector sensitivity, f_S is the frequency of the drive wave, and $b_1 + ib_2$ is the background. The resonance frequency F may be calculated after a series of the frequencies of the source wave and amplitudes of the detected wave are measured.

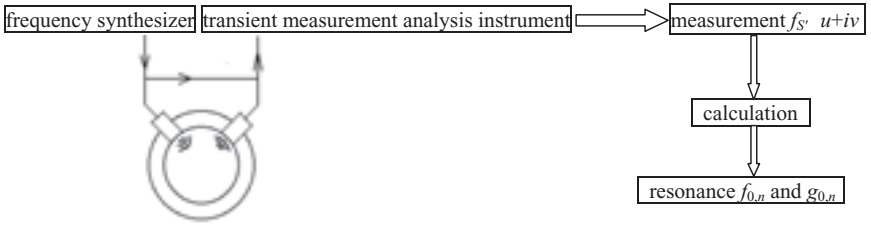

Fig. 1. Measurement principle of speed of sound in gas with spherical resonator.

Considering the practical factor, the speed of sound u is determined with the following expression:

$$\mathsf{F} = f_{0,s} + ig_{0,s} = \frac{uv_{0,s}}{2\pi a} + \sum_{N} (\Delta f_N + ig_N) \tag{5}$$

where $(\Delta f + ig)$ includes the perturbation terms, and describes the deviations of the measured frequency from the ideal condition, which have been carefully discussed by Mehl and Moldover [3]. In the present measurements, the following three major perturbation terms including the bulk loss term, the shell correction term, and a thermal boundary layer term are taken into consideration.

Considering the energy dissipation of the acoustic wave in the processing of the propagation, the bulk loss term is corrected as

$$\Delta f_{\text{dis}} + ig_{\text{dis}} = i\frac{\pi^2 f_{0,s}^3}{c^2}\left[(\gamma - 1)\,\delta_t^2 + \frac{4}{3}\delta_v^2 + \frac{\eta_b}{\rho\omega}\right] \tag{6}$$

where δ_t is the thickness of the thermal boundary layer, $\delta_t = \sqrt{2D_t/\omega}$, and D_t is the thermal diffusivity. δ_v is the thickness of the viscous boundary layer, $\delta_v = \sqrt{2D_v/\omega}$, D_v is the viscous diffusivity, $D_v = \eta/\rho$, and η_b is the second viscosity, $\eta_b = 1/3\eta$, where η is the viscosity. For example, in the present work, the magnitude of the bulk loss term $g_{\text{dis}}/f_{0,2}$ for HCFC-22 at 293.598 K and 649.1 kPa is 1.3×10^{-4} when the resonance mode is (0,2).

The shell correction term caused by the elasticity of the shell wall of the spherical acoustic resonator is represented by

$$\Delta f_{\text{sh}} + ig_{\text{sh}} = \frac{1 + 2t^3}{2(t^3 - 1)}\frac{\rho u^2}{\rho_{\text{sh}} u_{\text{sh}}^2}\frac{f_{0,s}}{1 - (f_{0,s}/f_{\text{br}})^2} \tag{7}$$

where $t = b/a$ with an inner radius a and an outer radius b of the shell. ρ_{sh} is the density of the shell material, u_{sh} is the speed of longitudinal waves

in the shell material, and f_{br} is the breathing-mode resonance frequency, which is given by

$$f_{\mathrm{br}} = \sqrt{\frac{t^3-1}{2\pi^2(t-1)(1+2t^3)}}\left(\frac{u_{\mathrm{sh}}}{a}\right) \tag{8}$$

For example, the frequency shift $\Delta f_{\mathrm{sh}}/f_{0,2}$ for HCFC-22 at 293.598 K and 649.1 kPa is 9.6×10^{-5} when the resonance mode is (0,2).

The propagation of the acoustic wave is substantially assumed to be an adiabatic process, however, it becomes an isothermal process on the inner surface of the shell of the spherical resonator. Such a thermal boundary layer is corrected as follows:

$$\Delta f_{\mathrm{th}} + i g_{\mathrm{th}} = f_{0,s}\left[(1+i)\frac{\gamma-1}{2}\frac{\delta_t}{a} + (\gamma-1)\frac{u_{\mathrm{sh}}}{\omega}\frac{\lambda_g}{\lambda_{\mathrm{sh}}} + (\gamma-1)\frac{l_a}{a}\right] \tag{9}$$

The first term on the right-hand side of Eq. (9) is the usual thermal boundary layer term, whereas the second term is the correction for the effect of curvature of the wall surface, which is usually sufficiently small in comparison with the first term, and λ is the thermal conductivity. The third term represents the temperature jump effect, where l_a is the thermal accommodation length and is expressed as

$$l_a = \frac{\lambda}{p}\sqrt{\frac{\pi MT}{2R}}\frac{(2-h)/h}{c_v/R+1/2} \tag{10}$$

where c_v is the isochoric specific heat capacity, and h is the thermal accommodation coefficient and is approximately equal to 1.

For example, the frequency shift $\Delta f_{\mathrm{th}}/f_{0,2}$ and the loss $g_{\mathrm{th}}/f_{0,2}$ for HCFC-22 at 293.598 K and 649.1 kPa are 1.1×10^{-5} and 4.3×10^{-5}, respectively, when the resonance mode is (0,2).

For a real gas, the speed of sound in the gaseous phase can be written as a function of the pressure p and temperature T, similar to the virial equation of state:

$$u^2 = \left(\frac{\partial p}{\partial \rho}\right)_s = \frac{\gamma^0 RT}{M}\left[1 + \frac{\beta_a}{RT}p + \frac{\gamma_a}{RT}p^2 + \frac{\delta_a}{RT}p^3 + \cdots\right] \tag{11}$$

where $\gamma^0 = c_p^0/c_v^0$ is the ratio of the isobaric to isochoric ideal-gas heat capacity. M is the molar mass, and R is the universal gas constant, $R = 8.314471\ \mathrm{J\cdot mol^{-1}\cdot K^{-1}}$. β_a, γ_a, δ_a,... are the second, third, and fourth acoustic virial coefficients, respectively, and they are functions of the temperature T only.

At the various pressures and temperatures, the speeds of sound were determined using Eq. (5), and were represented as a function of pressure by

$$u^2 = c_0 + c_1 p + c_2 p^2 + \cdots \qquad (T = \text{constant}) \tag{12}$$

where c_0, c_1, c_2,... are numerical fitted parameters. Comparing the first term on the right-hand side of Eq. (12) with that of Eq. (11), a relationship was obtained:

$$\gamma^0 = \frac{M}{RT} c_0 \tag{13}$$

A relationship between γ^0 and c_p^0 is given as follows:

$$c_p^0 = \frac{\gamma^0}{\gamma^0 - 1} R \tag{14}$$

Thus, the ideal-gas isobaric heat capacity c_p^0 at a certain temperature may be determined, and the second acoustic virial coefficient β_a can be obtained by the same method for the second term on the right-hand side of Eqs. (11) and (12):

$$\beta_a = RT \frac{c_1}{c_0} \tag{15}$$

3. EXPERIMENTAL APPARATUS AND PROCEDURES

A schematic of the experimental apparatus to measure the speed of sound with a spherical acoustic resonator used in the present study is shown in Fig. 2. The experimental apparatus consists of an experimental cell, a signal measuring system, a temperature controlling and measuring system, a pressure measurement system, and a vacuum and gas-supplying system. As illustrated in Fig. 2, the experimental cell consisted of a spherical acoustic resonator A and a pressure vessel B. The signal measuring system consisted of a frequency synthesizer H, a drive transducer M_1, a detection transducer M_2, and a transient measurement analysis instrument I. The temperature controlling and measuring system consisted of a thermostated bath P, a temperature controlling and heating unit N, and a temperature-measuring unit M. The pressure measurement system J consisted of a pressure gauge and a dead-weight pressure gauge. The vacuum system consisted of a vacuum pump and a vacuum-measuring gauge. The spherical acoustic resonator placed in the pressure vessel was immersed in the

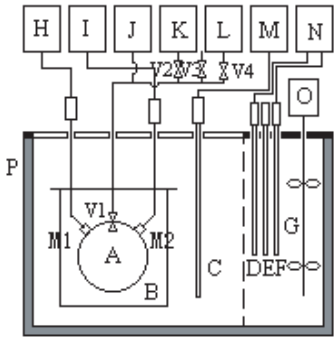

A: Spherical resonator; B: Pressure vessel; C: Platinum resistance thermometer;
D: Auxiliary heater; E: Resistance; F: Main heater; G: Stirrer;
H: Frequency synthesizer; I: Transient measurement analysis instrument:
J: Pressure measurement system; K: Vacuum system; L: Sample vessel
M: Temperature-measuring instrument; M_1, M_2: Transducers;
N: Temperature controlling system O: Solenoid motor;
P: Thermostated bath; V_1~V_4: Valves

Fig. 2. Experimental system for speed-of-sound measurements of gases.

thermostated bath filled with the water, and the substance to be investigated was charged into the spherical acoustic resonator and the pressure vessel.

The spherical acoustic resonator used in this study was assembled from two hemispheres that are made of the Type 00Cr17Ni14Mo2 stainless steel. Its inner radius, which was determined with a coordinate measuring machine, is about 61.77 mm at 20°C. The drive and detection transducers were designed and manufactured by the Acoustic Research Institute of Academy of Science of China, and their working frequencies are between 1 and 15 kHz in this study.

After confirming the thermal equilibrium condition, the temperature of the gas was measured with a 25-Ω standard platinum resistance thermometer, the pressure was measured with a pressure gauge and a dead-weight pressure gauge, and the amplitudes of the sound wave were measured and processed by the transient measurement analysis instrument. At a prescribed temperature and pressure, we completed a series of measurements for all resonant modes when the frequencies were increased and decreased in steps of 0.1 Hz three times. Next, the pressure was reduced at

constant temperature for the next measurement. In this study, speeds of sound for each substance were measured along four isotherms.

4. DETERMINATION OF RESONATOR RADIUS

The deduction of the speed of sound from Eq. (5) required a knowledge of the inner radius a of the spherical resonator as a function of temperature. The radius of the resonator is determined accurately through measurements using a monatomic gas. For unknown a, the value u/a from Eq. (5) at various pressures and temperatures could be obtained, and were similarly represented as a function of pressure with an equation like Eq. (12). Thus, Eq. (13) was also obtained. For a monatomic gas, the specific heat ratio $\gamma_0 = 3/5$, and the inner radius a included in the constant c_0 can be calculated from Eq. (13). Argon was chosen as the monatomic gas to determine the inner radius in the present study, because the speed of sound of argon is about 300 $\mathrm{m \cdot s^{-1}}$, which means that there are five radially symmetric modes within the range of measurable frequencies, and the physical properties of argon are well known. The physical properties used to evaluate the perturbation terms for argon are from Ref. 3. The mass purity of argon used in the present study is better than 99.999%.

Along four different isotherms, 28 speeds of sound of argon were measured, while the inner radius a of the spherical acoustic resonator was correlated by the function of temperature given below:

$$a = 61.5765 + 6.75793 \times 10^{-4} T \tag{16}$$

where a is in mm and T is in K. The inner radius from the measurements and Eq. (16) is shown in Fig. 3.

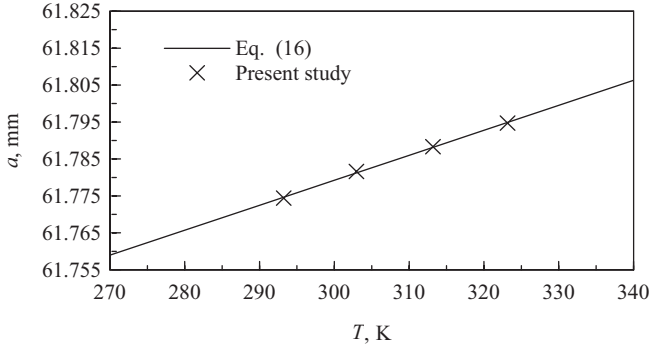

Fig. 3. Spherical resonator radius from measurements for Ar and Eq. (16).

Table I. Experimental Uncertainties for Temperature, Pressure, and Speed of Sound

Temperature	Platinum resistance thermometer, u_1:	6.8 mK
	Thermometer bridge, u_2:	0.5 mK
	Temperature stability of thermostated bath, u_3:	1.0 mK
	Combined standard uncertainty, u_c:	6.9 mK
Pressure	Dead weight pressure gauge, u_1:	0.98 kPa
	Differential pressure detector, u_2:	0.08 kPa
	Atmospheric pressure gauge, u_3:	0.04 kPa
	Combined standard uncertainty, u_c:	0.98 kPa
Speed of sound	Inner radius of the spherical resonator, u_1:	18.7 ppm
	Signal measurement, u_2:	1 ppm
	Combined standard uncertainty, u_c:	18.7 ppm

5. EXPERIMENTAL UNCERTAINTIES

According to ISO (International Organization for Standardization) guidelines for the experimental uncertainty, the extended uncertainty U of the measured values can be calculated by the following equation:

$$U = k u_c = k \sqrt{\sum (u_i)^2} \tag{17}$$

where u_i is the standard uncertainty and subscript i is the component of the uncertainty, u_c is the combined uncertainty, k is the coverage factor, and is usually taken as 2 or 3. In the present study, the coverage factor k is taken as 2, and the level of confidence corresponds to 95%. Table I lists the standard uncertainties and the combined uncertainties. The experimental uncertainties in temperature, pressure, and speed-of-sound measurements are estimated to be not greater than ± 14 mK, ± 2.0 kPa, and $\pm$ 0.0037%.

6. RESULTS

6.1. Chlorodifluoromethane (HCFC-22)

The speeds of sound in gaseous HCFC-22 were measured for the pressure range from 200 to 650 kPa along four isotherms at 293, 303, 313, and 323 K. The results are given in Table II. The purity of the HCFC-22 sample is better than 99.95 mass%, which was analyzed by the manufacturer. The thermophysical properties, such as the viscosity, thermal conductivity and density, used in the correction terms of the resonant frequencies, are from Refs. 13–15. The ideal-gas isobaric specific heat capacity c_p^0 and the second acoustic virial coefficient β_a have been determined from the present measurements as given in Table III. The present c_p^0 values together

Table II. Speed-of-Sound Data for Gaseous HCFC-22

T (K)	p (kPa)	u (m·s^{-1})	T (K)	p (kPa)	u (m·s^{-1})
293.598	649.1	168.952	302.962	631.6	173.258
	593.1	170.306		591.9	174.079
	494.5	172.355		496.1	175.858
	398.5	174.371		398.2	177.765
	301.1	176.356		300.4	179.497
	203.3	178.243		199.4	181.248
313.176	631.1	177.315	323.163	630.5	181.000
	593.0	177.998		592.4	181.671
	494.8	179.722		495.2	183.164
	397.8	181.334		398.2	184.629
	300.5	182.918		300.4	186.043
	203.0	184.409		203.4	187.403

Table III. Ideal-Gas Isobaric Specific Heat Capacity and Second Acoustic Virial Coefficient for HCFC-22

T (K)	c_p^0/R	β_a (cm^3·mol^{-1})
293.598	6.786	−471.900
302.962	6.922	−432.224
313.176	7.033	−385.292
323.163	7.160	−352.105

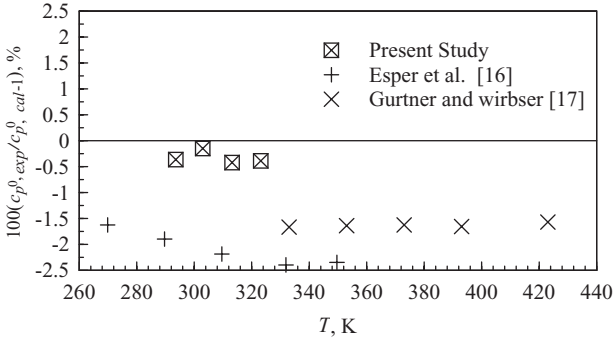

Fig. 4. Deviations of c_p^0 for HCFC-22 from McLinden correlation [18].

Table IV. Speed-of-Sound Data for Gaseous HFC-152a

T (K)	p (kPa)	u (m·s^{-1})	T (K)	p (kPa)	u (m·s^{-1})
293.864	415.6	192.686	302.962	412.5	197.004
	376.3	193.984		377.2	198.005
	340.0	195.186		337.3	199.200
	301.1	196.387		300.5	200.297
	260.2	197.690		260.6	201.398
	202.7	199.482		203.3	202.997
313.186	415.2	200.942	323.163	415.8	205.476
	377.7	201.936		377.1	206.175
	338.2	202.948		338.5	207.271
	300.5	203.930		301.0	208.170
	261.2	204.951		260.4	209.168
	202.6	206.435		203.0	210.320

with those recently reported by Esper et al. [16] and Gurtner and Wirbser [17] are compared with the correlation developed by McLinden [18] in Fig. 4. Esper et al. reported c_p^0 values of HCFC-22 for which the purity is only 99.5% with the same measurement method, and Gurtner and Wirbser obtained c_p^0 with a flow calorimeter. All measured c_p^0 data are lower than the McLinden correlation, and the present c_p^0 values agree with this correlation within 0.5%.

6.2. Pentafluoroethane (HFC-152a)

The speeds of sound in gaseous HFC-152a were measured for the pressure range from 200 to 420 kPa along four isotherms at 293, 303, 313, and 323 K. The results are given in Table IV. The purity of the HFC-152a sample is better than 99.95 mass%, which was analyzed by the manufacturer. The thermophysical properties, such as the viscosity, thermal conductivity and density, used in the correction terms of the resonant frequencies, are from Refs. 19 and 20. The ideal-gas isobaric specific heat capacity c_p^0 and the second acoustic virial coefficient β_a have been determined from the present measurements as given in Table V.

Gillis [21], Hozumi et al. [6], and Beckermann and Kohler [5] have also determined the c_p^0 of HFC-152a through speed-of-sound measurements, Hozumi et al. and Beckermann and Kohler used the same method as the present study, but Gillis used a cylindrical acoustic resonator to measure the speed of sound. The purity of the sample used by Beckermann and Kohler is only 99.7%. A dimensionless c_p^0 correlation based on

Table V. Ideal-Gas Isobaric Specific Heat Capacity and Second Acoustic Virial Coefficient for HFC-152a

T (K)	c_p^0/R	β_a ($cm^3 \cdot mol^{-1}$)
293.864	8.077	−678.704
302.962	8.298	−597.547
313.186	8.433	−545.709
323.163	8.593	−485.831

the present c_p^0 together with the values reported by Gillis and Hozumi et al. was developed as

$$c_p^0/R = 2.28355 + 8.06736T_r - 0.612881T_r^2 \tag{18}$$

where $T_r = T/T_c$, and the range of application is from 240 to 400 K.

Figure 5 shows the deviations among the four sets of c_p^0 values, the Hozumi et al. correlation [5], the McLinden correlation [18], and the above correlation. The present c_p^0 values agree well with the other values expect for the Beckermann and Kohler values at high temperatures.

6.3. 1,1,1-Trifluoroethane (HFC-143a)

The speeds of sound in gaseous HFC-143a were measured for the pressure range from 200 to 800 kPa along four isotherms at 293, 303, 313, and 323 K. The results are given in Table VI. The purity of the HFC-143a

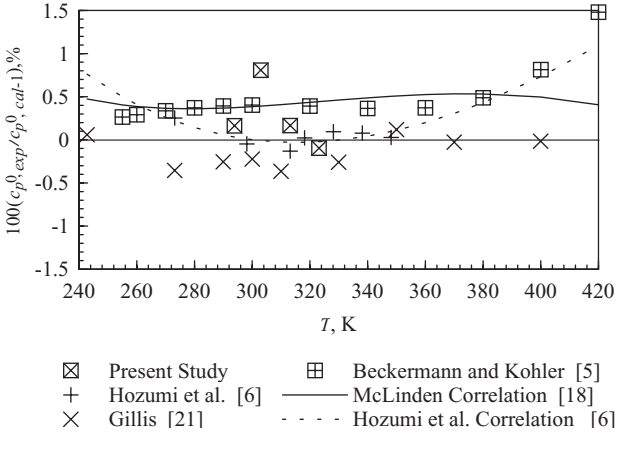

Fig. 5. Deviations of c_p^0 for HFC-152a from Eq. (18).

Table VI. Speed-of-Sound Data for Gaseous HFC-143a

T (K)	p (kPa)	u (m·s^{-1})	T (K)	p (kPa)	u (m·s^{-1})
293.608	787.2	161.116	302.962	787.0	166.054
	690.8	163.817		689.1	168.346
	592.4	166.129		593.2	170.656
	495.5	168.819		495.3	172.847
	398.0	171.225		397.6	174.945
	300.7	173.522		301.0	177.044
	202.7	175.823		202.9	179.047
313.186	787.6	170.727	323.183	787.0	174.907
	690.0	172.717		690.4	176.701
	592.5	174.726		592.7	178.460
	494.8	176.722		495.4	180.206
	398.2	178.541		397.6	181.899
	300.5	180.431		300.4	183.507
	203.4	182.218		203.1	185.259

sample is better than 99.95 mass%, which was analyzed by the manufacturer. The thermophysical properties, such as the viscosity, thermal conductivity and density, used in the correction terms of the resonant frequencies, are from Ref. 5. The ideal-gas isobaric specific heat capacity c_p^0 and the second acoustic virial coefficient β_a have been determined from the present measurements as given in Table VII.

The c_p^0 of HFC-143a was also reported by Beckermann and Kohler [5] and Gillis [21] through speed-of-sound measurements with acoustic spherical and cylindrical resonators, respectively. The purity of the sample used by Beckermann and Kohler was only 99.3%. A dimensionless c_p^0 correlation based on the present c_p^0, together with those of the Gillis, was developed as

$$c_p^0/R = 1.44449 + 11.1771T_r - 2.27109T_r^2 \tag{19}$$

where the range of application is from 250 to 400 K.

Table VII. Ideal-Gas Isobaric Specific Heat Capacity and Second Acoustic Virial Coefficient for HFC-143a

T (K)	c_p^0/R	β_a (cm^3·mol^{-1})
293.608	9.288	−566.579
302.962	9.485	−525.243
313.186	9.696	−490.541
323.183	9.899	−465.925

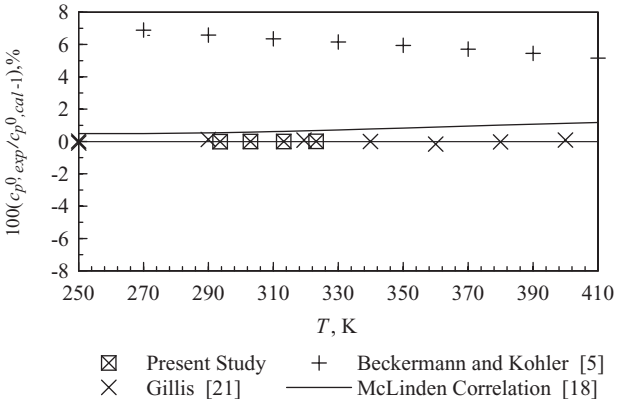

Fig. 6. Deviations of c_p^0 for HFC-143a from Eq. (19).

Figure 6 shows the deviations among the three sets of c_p^0 values, the McLinden correlation [18], and the above correlation. The present c_p^0 values agree well with those of Gillis; the Beckermann and Kohler c_p^0 values are higher than Eq. (19) by 6% or so.

6.4. Propane (HC-290)

The speeds of sound in gaseous propane were measured for the pressure range from 200 to 700 kPa along four isotherms at 293, 303, 313, and 323 K. The results are given in Table VIII. The purity of the propane

Table VIII. Speed of Sound Data for Gaseous Propane

T (K)	p (kPa)	u (m·s^{-1})	T (K)	p (kPa)	u (m·s^{-1})
293.480	668.2	224.860	302.962	668.6	230.999
	592.3	228.158		592.8	233.802
	495.7	232.055		494.6	237.427
	397.6	235.953		397.0	240.829
	300.0	239.549		300.7	244.113
	202.9	243.147		203.5	247.315
313.206	669.3	236.967	323.193	669.3	242.730
	592.5	239.589		592.9	244.925
	495.3	242.716		495.1	247.824
	398.4	245.238		397.4	250.523
	300.0	248.767		300.5	253.222
	202.8	251.696		203.6	255.819

Table IX. Ideal-Gas Isobaric Specific Heat Capacity and Second Acoustic Virial Coefficient for Propane

T (K)	c_p^0/R	β_a ($cm^3 \cdot mol^{-1}$)
293.480	8.707	−636.185
302.962	8.891	−601.168
313.206	9.162	−559.403
323.193	9.403	−523.370

sample is better than 99.95 mass%, which was analyzed by the manufacturer. The thermophysical properties, such as the viscosity, thermal conductivity, and density, used in the correction terms of the resonant frequencies, are from Ref. 22. The ideal-gas isobaric specific heat capacity c_p^0 and the second acoustic virial coefficient β_a have been determined from the present measurements as given in Table IX.

The c_p^0 of propane wase reported by Esper et al. [23] and Trusler and Zarari [24] through speed of sound measurements with spherical acoustic resonators. A dimensionless c_p^0 correlation based on the present c_p^0 values, together with those of Esper et al. and Trusler and Zarari, was developed as

$$c_p^0/R = 3.20946 + 5.40615T_r + 1.89922T_r^2 \tag{20}$$

where the range of application is from 225 to 375 K.

Figures 7 shows the deviations among the three sets of c_p^0 values, the Trusler and Zarari correlation [24] and the above correlation. The present

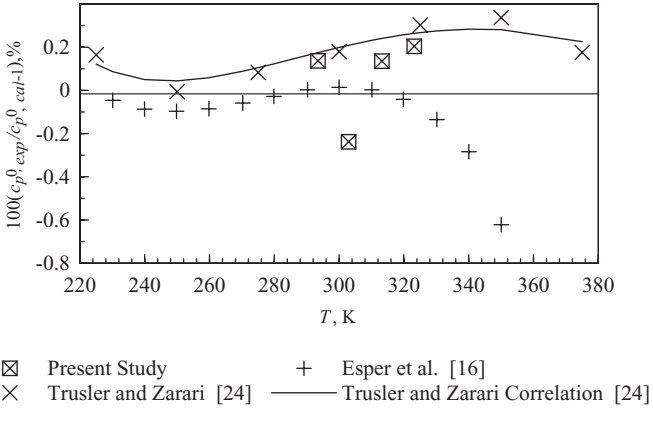

Fig. 7. Deviations of c_p^0 for propane from Eq. (20).

c_p^0 values agree well with those of Trusler and Zarari, and the Esper c_p^0 values are lower than Eq. (20) at high temperatures.

7. CONCLUSION

Speeds of sound, ideal-gas heat capacities, and second acoustic virial coefficients have been experimentally studied for chlorodifluoromethane (HCFC-22), pentafluoroethane (HFC-152a), 1,1,1-trifluoroethane (HFC-143a), and propane (HC-290) with a spherical acoustic resonator. Twenty-four speed-of-sound values in gaseous HCFC-22 were measured for pressures from 200 to 650 kPa along four isotherms at 293.598, 302.962, 313.176, and 323.163 K. Twenty-four speed-of-sound values in gaseous HFC-152a were measured for pressures from 200 to 420 kPa along four isotherms at 293.864, 302.962, 313.186, and 323.163 K. Twenty-eight speed-of-sound values in gaseous HFC-143a were measured for pressures from 200 to 800 kPa along four isotherms at 293.608, 302.962, 313.186 and 323.183 K. Twenty-four speed-of-sound values in gaseous propane were measured for pressures from 200 to 670 kPa along four isotherms at 293.480, 302.962, 313.206, and 323.193 K. The experimental uncertainties of temperature, pressure, and speed of sound are estimated to be ± 14 mK, 2.0 kPa, and $\pm 0.0037\%$, respectively.

The ideal-gas isobaric heat capacities as well as the second acoustic virial coefficients for these substances have been deduced from the present speed-of-sound measurements. Equations of ideal-gas specific heat capacities for HFC-152a, HFC-143a, and propane are also proposed.

ACKNOWLEDGMENTS

This work was supported by the National Natural Science Foundation of China (Grant 50106009). The authors would like to thank Dr. K. Zeng for his assistance with the experimental work, and we are grateful to Zhejiang Fluoro-Chemical Technology Research Institute for providing the experimental samples.

REFERENCES

1. M. J. Molina and F. S. Rowland, *Nature* **249**:810 (1974).
2. M. R. Moldover, M. Waxman, and M. Greespan, *High Temp.-High Press* **11**:75 (1979).
3. M. R. Moldover, J. B. Mehl, and M. Greenspan, *J. Acoust. Soc. Am.* **79**:253 (1986).
4. M. B. Ewing, M. L. McGlashan, and J. P. M. Tusler, *Metrologia* **22**:93 (1986).
5. W. Beckerman and F. Kohler, *Int. J. Thermophys.* **16**:455 (1995).
6. T. Hozumi, T. Koga, H. Sato, and K. Watanabe, *Int. J. Thermophys.* **14**:739 (1993).
7. Z. G. Liu, in *Proc. 18th Japan Symp. Thermophys. Props.* (Nara, 1997), p. 7.

8. M. G. He, Z. G. Liu, X. M. Zhao, and J. M. Yin, *J. Xi'an Jiaotong University* **34**:35 (2000) [in Chinese].
9. M. G. He, Ph.D. Dissertation (School of Energy and Power Engineering, Xi'an Jiaotong University, Xi'an, China, 1999).
10. M. G. He and Z. G. Liu, *Fluid Phase Equil.* **198**:185 (2002).
11. M. R. Moldover, J. P. M. Trusler, T. J. Edwards, J. B. Mehl, and R. S. Davis, *J. Rest. Natl. Bur. Stand. (U.S.)* **93**:85 (1988).
12. J. B. Mehl, *J. Acoust. Soc. Am.* **64**:1523 (1978).
13. J. M. Yin and M. G. He, *J. Xi'an Jiaotong University* **28**:23 (1994) [in Chinese].
14. T. Makita, Y. Tanaka, Y. Noguchi, and H. Kubota, *Int. J. Thermophys.* **2**:249 (1981).
15. W. Wagner, V. Marx, and A. Pruß, *Int. J. Refrig.* **16**:373 (1993).
16. G. Esper, W. Lemming, W. Beckermann, and F. Kohler, *Fluid Phase Equil.* **105**:173 (1995).
17. J. Gurtner and H. Wirbser, *J. Chem. Thermodyn.* **29**:1205 (1997).
18. M. O. McLinden, *Int. J. Refrig.* **13**:149 (1990).
19. R. Krauss, V. C. Weiss, T. A. Edison, J. V. Sengers, and K. Stephan, *Int. J. Thermophys.* **17**:731 (1996).
20. T. Tamatsu, H. Sato, and K. Watanabe, *Int. J. Refrig.* **16**:347 (1993).
21. K. A. Gillis, *Int. J. Thermophys.* **18**:73 (1997).
22. B. A. Younglove and J. F. Ely, *J. Phy. Chem. Ref. Data* **16**:577 (1987).
23. G. Esper, W. Lemming, W. Beckermann, and F. Kohler, *Fluid Phase Equil.* **105**:173 (1995).
24. J. P. M. Trusler and M. P. Zarari, *J. Chem. Thermodyn.* **28**:329 (1996).